Isoskeletal $Rh_{10}C_2$ Metal Clusters containing Four $Au(PPh_3)$ Groups and a Variable Number of Carbonyl Ligands‡

Alessandro Fumagalli,*,[a] Secondo Martinengo,[b] Vincenzo G. Albano,†,[c] Dario Braga[c] and Fabrizia Grepioni[c]

[a] *CNR–Centro di Studio sulla Sintesi e la Struttura dei Composti dei Metalli di Transizione nei Bassi Stati di Ossidazione, Via G. Venezian 21, I-20133 Milano, Italy*

[b] *Dipartimento di Chimica Inorganica, Metallorganica e Analitica dell'Università, Via G. Venezian 21, I-20133 Milano, Italy*

[c] *Dipartimento di Chimica 'G. Ciamician' dell'Università, Via Selmi 2, I-40126 Bologna, Italy*

The two new mixed-metal carbido–carbonyl clusters $[Rh_{10}C_2(CO)_{20}\{Au(PPh_3)\}_4]$ **1** and $[Rh_{10}C_2(CO)_{18}\{Au(PPh_3)\}_4]$ **2** have been obtained by reaction of $K_2[Rh_{12}C_2(CO)_{24}]$ with $[Au(PPh_3)Cl]$. The two molecules are in equilibrium through the dissociation–association of two carbonyl ligands. Phosphorus-31 NMR solution spectra of both compounds are reported. The molecular structures of both **1** and **2** have been determined by single-crystal X-ray diffraction. The compounds are isomorphous and crystallize in the tetragonal system, space group $P4_2/m$, $Z = 2$; $a = b = 15.446(3)$, $c = 21.894(2)$ Å for **1**, and $a = b = 15.400(5)$, $c = 21.801(5)$ Å for **2**. The molecules contain a close-packed $Rh_{10}C_2$ bioctahedral core with the carbide atoms filling the cavities. Four $Au(PPh_3)$ groups span triangular faces and the CO ligands cover the Rh_{10} polyhedron conforming to a D_{2h} idealized molecular symmetry.

In previous papers we have reported the synthesis and structural characterization in solution and/or solid state of several high-nuclearity mixed-metal clusters derived from the reaction of the trigonal-prismatic dianion $[Rh_6C(CO)_{15}]^{2-}$ [1] with electrophilic metal fragments such as $M(PPh_3)^+$ (M = Cu, Ag or Au),[2] $M(NCMe)^+$ (M = Cu or Ag)[2,3] and Ag^+.[4] The octahedral dianion $[Rh_6C(CO)_{13}]^{2-}$ [5,6] has also been found reactive toward $[Au(PPh_3)Cl]$, yielding $[Rh_6C(CO)_{13}\{Au_2(PPh_3)_2\}]$ [7] with an unusual Au–Au interaction. In all these species the heteroatom couples with the Rh polyhedron, whose geometry is essentially preserved, exclusively by capping one or two triangular faces. In order to extend these studies we have attempted the same kind of reactions on the higher nuclearity dianion $Rh_{12}C_2$ family of anions,[8] starting with $[Rh_{12}C_2(CO)_{24}]^{2-}$. Contrary to what has been previously observed, the reaction unpredictably results in the partial demolition of the rhodium polyhedron and rearrangement of the metal atoms around the two interstitial carbide atoms.

Results and Discussion

Synthesis and Chemical Characterization.—The reaction of $K_2[Rh_{12}C_2(CO)_{24}]$ with $[Au(PPh_3)Cl]$ takes place in several stages which may be partially tracked by IR spectroscopy as the gold complex is increasingly added to a solution of the cluster compound in tetrahydrofuran (thf) or propan-2-ol. Particularly, under a nitrogen atmosphere and with approximately a 1:1 molar ratio, a new cluster anion is observed in solution, together with some unreacted $[Rh_{12}C_2(CO)_{24}]^{2-}$. This species, presently uncharacterized, eventually becomes predominant with further addition of $[Au(PPh_3)Cl]$, while $[Rh_{12}C_2(CO)_{24}]^{2-}$ disappears. A larger excess of $[Au(PPh_3)Cl]$ causes formation of a fine brown-red precipitate and eventually only $[Rh(CO)_2Cl_2]^-$ remains in solution. The presence of this latter compound suggests a demolition process of the rhodium cluster induced by Cl^-.

Under CO at atmospheric pressure there is no IR spectroscopic evidence of intermediate stages, so that $[Rh(CO)_2Cl_2]^-$ and the precipitate apparently derive directly from the $[Rh_{12}C_2(CO)_{24}]^{2-}$ dianion. In any case, both under nitrogen and CO, the reaction is driven to completion when 4 moles of $[Au(PPh_3)Cl]$ have been added to the dianion and $[Rh_{10}C_2(CO)_{20}\{Au(PPh_3)\}_4]$ **1** is produced, almost quantitatively in thf, according to equation (1).

$$[Rh_{12}C_2(CO)_{24}]^{2-} + 4[Au(PPh_3)Cl] \longrightarrow \underset{\mathbf{1}}{[Rh_{10}C_2(CO)_{20}\{Au(PPh_3)\}_4]} + 2[Rh(CO)_2Cl_2]^- \quad (1)$$

It was difficult to characterize this fine amorphous powder as any attempt at purification and crystallization was hindered by its very low solubility in most common solvents (estimated in thf < 1 mg cm^{-3}). Only 1-methylpyrrolidin-2-one (mpo) proved suitable in which the powder showed a solubility of *ca.* 100 mg cm^{-3}.

We observed that dissolution of the crude product in mpo, under a nitrogen atmosphere, induces evolution of CO, detectable by IR spectroscopy, resulting in the formation of $[Rh_{10}C_2(CO)_{18}\{Au(PPh_3)\}_4]$ **2**. The same conversion into **2** was observed when the crude product precipitated from the reaction performed in propan-2-ol, which from IR spectroscopic evidence (Nujol mull) indicated a mixture of products.

The two species **1** and **2** are in equilibrium through the dissociation and association of two carbonyl ligands, according to equation (2).

$$\underset{\mathbf{1}}{[Rh_{10}C_2(CO)_{20}\{Au(PPh_3)\}_4]} \rightleftharpoons \underset{\mathbf{2}}{[Rh_{10}C_2(CO)_{18}\{Au(PPh_3)\}_4]} + 2CO \quad (2)$$

* For correspondence on synthesis and chemical characterization.
† For correspondence on structural characterization.
‡ *Supplementary data available:* see Instructions for Authors, *J. Chem. Soc., Dalton Trans.*, 1993, Issue 1, pp. xxiii–xxviii.

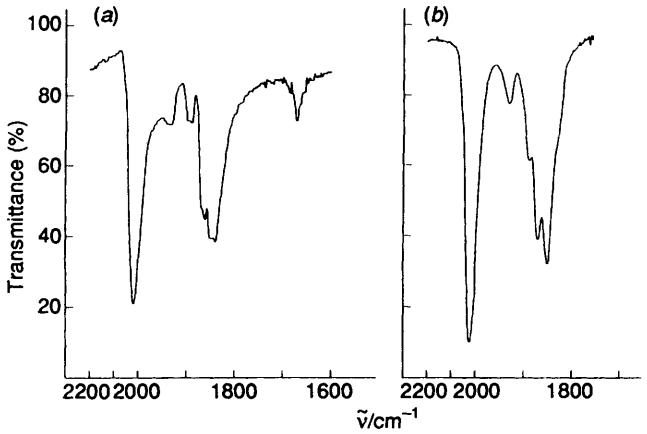

Fig. 1 Nujol mull (*a*) and mpo solution (*b*) IR spectra of $[Rh_{10}C_2(CO)_{20}\{Au(PPh_3)\}_4]$·mpo **1**

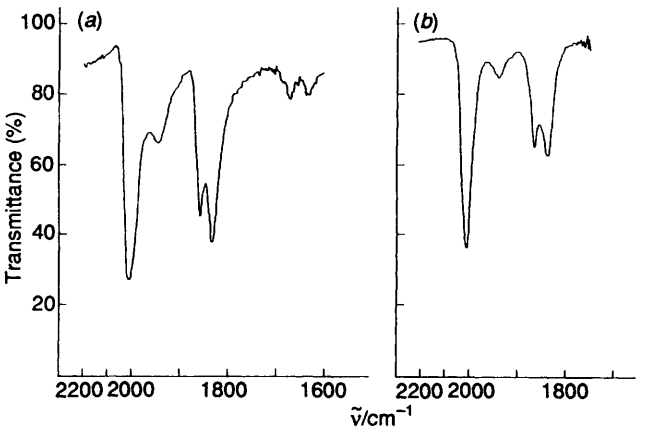

Fig. 2 Nujol mull (*a*) and mpo solution (*b*) IR spectra of $[Rh_{10}C_2(CO)_{18}\{Au(PPh_3)\}_4]$·mpo **2**

This reversible equilibrium is observed at room temperature under mild conditions, thus dissolution of **1** in mpo under a nitrogen atmosphere is enough to show, within minutes, the increasing formation of $[Rh_{10}C_2(CO)_{18}\{Au(PPh_3)\}_4]$ **2** with a change in colour from dark-red to brown; IR subtractive techniques gave no evidence of intermediate steps. Upon the application of a vacuum **2** becomes eventually the only species in solution. The process is reversed by the addition of CO [1–5 atm (100–500 kPa)] at room temperature. Spectroscopic evidence shows, within minutes, complete conversion to $[Rh_{10}C_2(CO)_{20}\{Au(PPh_3)\}_4]$ which may be recovered pure by precipitation. An mpo solution of **1** was essentially unchanged over 4 d under high CO pressures [40–100 atm (4–10 MPa)] at 5–10 °C, with only minor decomposition to an insoluble uncharacterized product. Gas volumetric measurements performed on pure, crystalline **2**, have confirmed the absorption of *ca.* 2 moles of CO per mole of product. Both **1** and **2**, according to elemental analyses and IR data (see below), crystallize with one molecule of clathrated mpo.

Spectroscopic Measurements.—The infrared spectra, in Nujol mull and mpo solution, of $[Rh_{10}C_2(CO)_{20}\{Au(PPh_3)\}_4]$·mpo **1** and $[Rh_{10}C_2(CO)_{18}\{Au(PPh_3)\}_4]$·mpo **2** are shown in Figs. 1 and 2, respectively. The bands (± 2 cm^{-1}) are at: **1** (Nujol mull) 2017s, 1938w, 1896w, 1888w, 1861m, 1849ms, 1839ms, 1686w and 1673w; (mpo solution) 2024s, 1930w, 1889mw, 1871m and 1851ms; **2** (Nujol mull) 2012s, 1946mw, 1860m, 1836ms, 1672w and 1637w; (mpo solution) 2012s, 1938w, 1863m and 1836ms cm^{-1}. The stretching bands at 1686–1673 and 1672–1634 cm^{-1} which are present in the Nujol-mull spectra [Fig. 1(*a*) and Fig. 2(*a*)], were assigned to the clathrated mpo solvent.

Natural abundance ^{13}C NMR at room temperature was not observed, probably due to the low concentration and/or spread

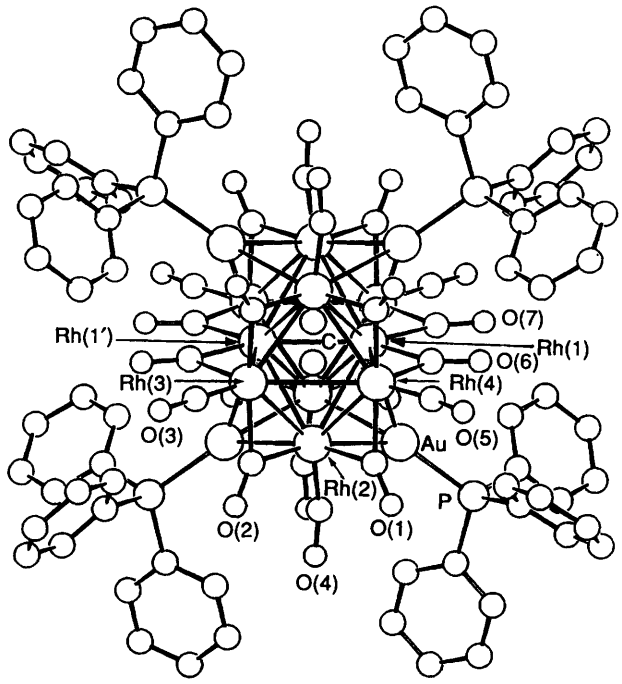

Fig. 3 The molecular stereogeometry of complex **1**. The molecule has crystallographic C_{2h} symmetry with the mirror plane containing the Rh_6C_2 equatorial grouping and eight CO ligands

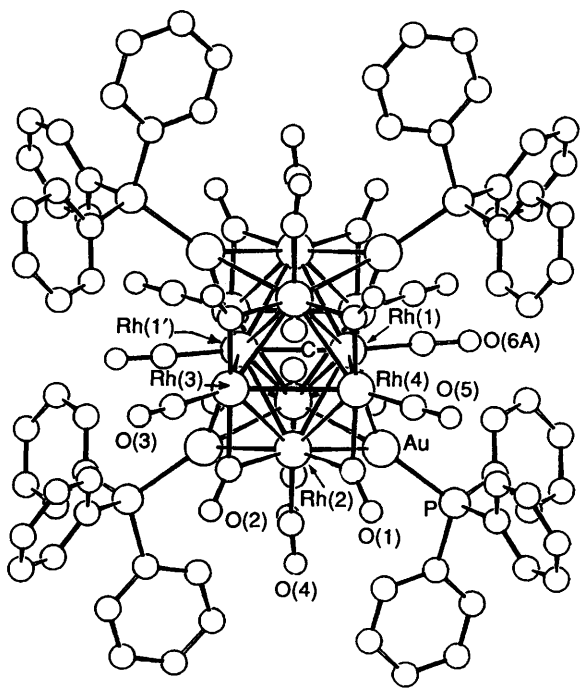

Fig. 4 The molecular stereogeometry of complex **2**. The metal atom polyhedron is the same as in **1** and the ligand coverage differs only for the equatorial C(6A)–O(6A) group, which shows some tendency towards bridging geometry and is disordered over two positions (only one of which is shown)

of the signals, ^{31}P NMR spectra were hardly detected being very broad and noisy: almost saturated solutions of **1** or **2** in mpo containing 15–20% $[^2H_6]$acetone, gave, within the temperature range 248–295 K, a broad doublet with $^2J_{P-Rh}$ *ca.* 14.8 Hz at δ 64.4 and an ill-defined peak at *ca.* δ 63.5 for **1** and **2**, respectively.

Structures of Compounds **1** *and* **2**.—The molecular geometries of **1** and **2** are shown in Figs. 3 and 4 respectively together with

Table 1 Selected bond distances (Å) for complexes **1** and **2**

Complex **1**				Complex **2**			
Rh(1)–Rh(4)	2.942(3)	Rh(4)–C(6)	2.04(2)	Rh(1)–Rh(4)	2.941(3)	Rh(1)–C(6A)	1.94(7)
Rh(1)–Rh(1′)	2.685(4)	Rh(1)–C(7)	2.07(2)	Rh(1)–Rh(1′)	2.651(3)	Rh(3) · · · C(7A)	2.87
Rh(1)–Rh(3′)	2.943(3)	Rh(3′)–C(7)	2.21(2)	Rh(1)–Rh(3)	2.931(3)	Rh(4) · · · C(6A)	2.86
Rh(2)–Rh(4)	2.785(2)	Rh(1)–C	2.01(3)	Rh(4)–Rh(2)	2.807(2)	Rh(1)–C	2.00(2)
Rh(2)–Rh(3)	2.788(2)	Rh(2)–C	2.05(1)	Rh(3)–Rh(2′)	2.804(2)	Rh(2)–C	2.05(1)
Rh(3)–Rh(4)	3.094(3)	Rh(3)–C	2.11(3)	Rh(3)–Rh(4′)	3.087(2)	Rh(3)–C	2.10(1)
Rh(1)–Rh(2)	3.031(2)	Rh(4)–C	2.11(2)	Rh(2)–Rh(1)	2.998(2)	Rh(4)–C	2.11(2)
Au–Rh(1)	2.757(1)	Au–P	2.293(5)	Au–Rh(1)	2.757(1)	Au–P	2.293(5)
Au–Rh(2′)	2.862(2)	P–C(8)	1.84(3)	Au–Rh(2″)	2.859(2)	P–C(8)	1.84(3)
Au–Rh(2)	2.858(2)	P–C(9)	1.84(3)	Au–Rh(2)	2.858(2)	P–C(14)	1.91(3)
Rh(2)–C(1)	2.05(2)	P–C(10)	1.86(3)	Rh(2)–C(1)	2.05(3)	P–C(20)	1.85(4)
Rh(4)–C(1)	2.04(2)	C(1)–O(1)	1.17(2)	Rh(3′)–C(1)	2.07(2)	C(1)–O(1)	1.17(3)
Rh(2)–C(2)	2.04(2)	C(2)–O(2)	1.18(2)	Rh(2)–C(2)	2.13(2)	C(2)–O(2)	1.17(3)
Rh(3)–C(2)	2.05(2)	C(3)–O(3)	1.21(2)	Rh(3)–C(2)	2.04(2)	C(3)–O(3)	1.08(4)
Rh(3)–C(3)	1.78(2)	C(4)–O(4)	1.21(2)	Rh(3)–C(3)	1.93(3)	C(4)–O(4)	1.08(3)
Rh(2)–C(4)	1.80(2)	C(5)–O(5)	1.22(2)	Rh(2)–C(4)	1.94(2)	C(5)–O(5)	1.16(5)
Rh(4)–C(5)	1.79(2)	C(6)–O(6)	1.21(2)	Rh(4)–C(5)	1.89(4)	C(7A)–O(7A)	1.18(6)
Rh(1)–C(6)	2.06(2)	C(7)–O(7)	1.20(2)	Rh(1)–C(7A)	1.91(5)	C(6A)–O(6A)	1.14(7)

their labelling schemes. In spite of the different stoichiometries the stereogeometries are so similar that the crystals turn out to be isomorphous. Selected bond distances and angles are given in Table 1. The geometric features of the two molecules are strictly comparable and will be discussed together. The relatively low quality of the diffraction data obtained in both cases (see Experimental section) allows us to establish and discuss only the general features of the two complexes.

The molecules contain a $Rh_{10}C_2$ core and four $Au(PPh_3)$ groups with the metal atoms closely packed. Twenty and eighteen CO groups complete the ligand coverage in **1** and **2** respectively. The $Rh_{10}C_2$ core is rather unique in the vast family of cluster compounds and it consists of two octahedra sharing an edge [Rh(1)–Rh(1′)], with the cavities occupied by carbon atoms (see Fig. 5). Six Rh atoms and the carbide atoms are strictly coplanar (equatorial plane). The four out-of-plane atoms, referred to as apical atoms [Rh(2) and symmetry equivalents], complete the octahedra and, together with the central atoms in the equator [Rh(1), Rh(1′)] define two tetrahedra fitted between the octahedra. The outer faces of the tetrahedra are capped by the Au atoms. This Rh-atom assemblage approximates a fragment of cubic close packing. The idealized symmetry of the $Rh_{10}C_2Au_4$ skeleton is D_{2h} but the molecules retain only precise C_{2h} symmetry in the crystal, with the mirror plane coincident with the equatorial plane. The differences in ligand arrangements in **1** and **2** are dictated by the need of accommodating two more ligands in **1**. The description is simpler in **2**, in which ten ligands are in terminal positions, one per rhodium atom and eight are in bridging geometry on the outer equator–apex edges. The CO ligands bonded to Rh(1) and Rh(1′) are slightly offset with respect to the Rh(1)–Rh(1′) direction, and are disordered over two sites with 50% occupancy. The disorder indicates a tendency towards edge-bridging geometry of these ligands. In fact in **1**, where two more CO groups are bonded, four ligands are allocated on the long edges of the equatorial rectangle (Fig. 5).

The Rh–C(carbide) distances range from 2.01(3) to 2.11(3) Å in **1** and from 2.00(2) to 2.11(2) Å in **2**, the C atoms being closer to the central Rh(1), Rh(1′) atoms than to the outer ones. The C(carbide) · · · C(carbide) separation is 2.98(2) and 2.99(2) Å in **1** and **2**, respectively. No appreciable swelling of the octahedral core in **1**, due to the larger number of electrons with respect to **2** (see below), can be detected.

The Rh–Rh bond lengths range from 2.685(4) to 3.094(3) Å in **1** and from 2.651(3) to 3.087(2) Å in **2**, the shortest bond corresponding, in both compounds, to the edge shared by the two octahedra and the longest being the outer unbridged equatorial bond.

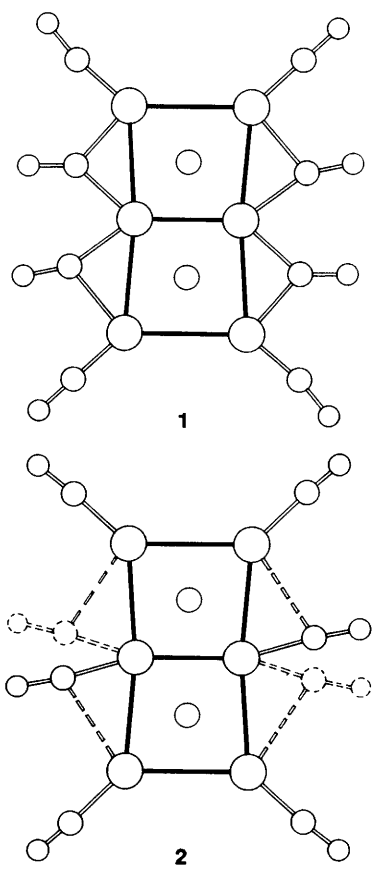

Fig. 5 The atoms in the equatorial plane of complexes **1** and **2** showing the relationship between the two species and the disordered CO ligands in **2** mimicking the situation in **1**

The Rh–Au bonds fall in a fairly narrow range [2.757(1)–2.862(2) Å in **1**, 2.757(1)–2.859(2) Å in **2**], the shortest bond being to Rh(1), the atom with the highest connectivity in the structure. The Rh–C(CO) and C–O bond distances in **1** average 1.79(2), 1.21(2) and 2.06(2), 1.19(2) Å for terminal and bridging ligands, respectively; the same bond distances in **2** average 1.93(4), 1.11(5) and 2.07(2), 1.17(3) Å for terminal and bridging carbonyls, respectively.

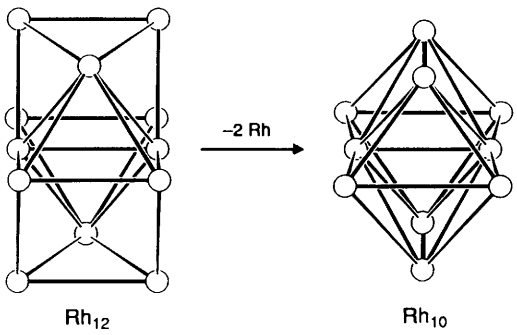

Fig. 6 The steric relationship between the Rh_{12} and Rh_{10} polyhedra suggesting the conversion mechanism (see text)

Conclusion

A challenge posed by cluster chemistry is the elucidation of the mechanisms of growth or transformation of the metal atom aggregates. Unfortunately acceptable rationalizations are very rarely possible. In the case of the $Rh_{12}C_2 \longrightarrow Rh_{10}C_2$ conversion a mechanism is suggested by the presence of Rh_6 planar arrangements in both metal atom clusters (two in Rh_{12} and one in Rh_{10} species, see Fig. 6). If one assumes that a likely mechanism implies minimum disruption and easy reorganization, the process should take place as follows: a planar Rh_6 unit remains substantially unaltered, while a $Rh(CO)_2^+$ fragment is eliminated from the upper and lower triangle (Fig. 6) as $[Rh(CO)_2Cl_2]^-$. The resultant Rh_{10} polyhedron rearranges in a closely packed form by movement of the remaining out-of-plane atoms, which remain attached to the equatorial plane. The new cluster, formally $[Rh_{10}C_2(CO)_{20}]^{4-}$, is stabilized further upon addition of four acidic $Au(PPh_3)^+$ fragments.

Another peculiar feature of the Rh_{10} species is that their stereogeometries change very little upon variation of two ligands (and four electrons). This is ascribed primarily to the possibility of confining the arrangements to the long edges of the equatorial rectangle, with no effect on the other ligands. But the steric features describe only part of the changes, the corresponding effects of electronic saturation of the metal atom cluster are of greater importance, though they do not produce detectable changes. This is where the four $Au(PPh_3)$ units play an important role; they stabilize **1** through a modulation of their accepting interactions.

Experimental

All operations were carried out under nitrogen or carbon monoxide as specified with a standard Schlenk-tube apparatus. Tetrahydrofuran was distilled from sodium–benzophenone and propan-2-ol from aluminium isopropoxide. 1-Methylpyrrolidin-2-one (mpo) and all other analytical grade solvents were degassed in vacuum and stored under nitrogen. The reagents $K_2[Rh_6C(CO)_{15}]\cdot x$thf ($x \approx 3$),[9] $K_2[Rh_{12}C_2(CO)_{24}]$[8a] and $[Au(PPh_3)Cl]$[10] were prepared by the published methods. Infrared spectra were recorded on a Perkin-Elmer 781 grating spectrophotometer equipped with 6800 Data Station for spectra elaboration, using 0.1 mm CaF_2 cells previously purged with nitrogen or CO; ^{31}P NMR spectra were recorded at 81.0 MHz on a Bruker AC200 instrument, with a resolution of ± 1.7 Hz.

Synthesis of $[Rh_{10}C_2(CO)_x\{Au(PPh_3)\}_4]$ (x = 18 *or* 20) *from* $K_2[Rh_6C(CO)_{15}]\cdot x$thf ($x \approx 3$) *and* $[Au(PPh_3)Cl]$.—This is a two-step preparation, in which $[Rh_{12}C_2(CO)_{24}]^{2-}$ is conveniently prepared *in situ*[10] and then treated with the gold complex. In a typical preparation a solution of $K_2[Rh_6C(CO)_{15}]\cdot x$thf (2886 mg, 2.15 mmol) in propan-2-ol (50 cm^3), was treated with aqueous H_2SO_4 (1 mol dm^{-3}, 2.25 cm^3) and heated under nitrogen at 70 °C for *ca.* 2 h. The resulting brown solution, checked by IR spectroscopy was assumed to be *ca.* 0.02 mol dm^{-3} in $K_2[Rh_{12}C_2(CO)_{24}]$. To 15 cm^3 of this solution (*ca.* 0.3 mmol), under a CO atmosphere, was added $[Au(PPh_3)Cl]$ (594.6 mg, 1.2 mmol) and propan-2-ol (5 cm^3). Within 2 h of stirring, a fine brick-red precipitate was formed and the IR spectrum of the decanted solution showed essentially only $[Rh(CO)_2Cl_2]^-$ (bands at 2074 and 2004 cm^{-1}) to be present. The precipitate was filtered, washed with propan-2-ol (2 × 5 cm^3), water (3 × 10 cm^3), again with propan-2-ol (2 × 5 cm^3), vacuum dried and stored under N_2.

The cluster $[Rh_{10}C_2(CO)_{20}\{Au(PPh_3)\}_4]$ **1** was obtained by dissolving the crude product (above) under a CO atmosphere in mpo (7 cm^3) and by careful layering with propan-2-ol (35 cm^3). When the diffusion was complete (*ca.* 2 weeks) the mother-liquor was removed by syringe and the precipitate washed thoroughly with propan-2-ol to remove the fine powder in suspension accompanying the large black crystals which were vacuum dried. As indicated by elemental analysis, the product crystallizes with one molecule of mpo (M = 3493.42). Yield: 800 mg, 75% {Found: C, 33.85; H, 2.00; N, 0.45. Calc. for $[Rh_{10}C_2(CO)_{20}\{Au(PPh_3)\}_4]\cdot C_5H_9NO$: C, 33.50; H, 1.95; N, 0.40%}.

If evacuation, followed by admission of a nitrogen atmosphere, over the solution of the crude product in mpo is employed instead $[Rh_{10}C_2(CO)_{18}\{Au(PPh_3)\}_4]$ **2** is obtained, which as above can be isolated upon layering with propan-2-ol.

Synthesis of $[Rh_{10}C_2(CO)_x\{Au(PPh_3)\}_4]$ (x = 18 *or* 20) *from* $K_2[Rh_{12}C_2(CO)_{24}]\cdot x$thf ($x \approx 2$) *and* $[Au(PPh_3)Cl]$.—The cluster salt $K_2[Rh_{12}C_2(CO)_{24}]\cdot x$thf ($x \approx 2$) (850.0 mg, 0.395 mmol) and $[Au(PPh_3)Cl]$ (776.2 mg, 1.569 mmol) were placed in a Schlenk tube under nitrogen and thf (20 cm^3) was added. The fine brick-red precipitate obtained within 4 h was filtered, washed with thf (3 × 5 cm^3) and vacuum dried. The crude product was redissolved in mpo (8 cm^3) and pumped *in vacuo* for *ca.* 45 min and then carefully layered with propan-2-ol (25 cm^3). When the slow diffusion was completed, the mother-liquor was removed with a syringe and the product was washed thoroughly with propan-2-ol to remove the fine powder in suspension accompanying the large crystals. As indicated by elemental analysis, the product crystallizes with one molecule of mpo. Yield of **2**: 950 mg (69%) of large black octahedral crystals {Found: C, 33.45; H, 1.75; N, 0.45. Calc. for $[Rh_{10}C_2(CO)_{18}\{Au(PPh_3)\}_4]\cdot C_5H_9NO$: C, 33.35; H, 2.00; N, 0.40%}.

This procedure also applied to the preparation of $[Rh_{10}C_2(CO)_{20}\{Au(PPh_3)\}_4]$ **1** if the crude product is recrystallized under a CO atmosphere.

X-Ray Crystal Structure Determination of Complexes **1** *and* **2**.—Crystal data and details of measurements for complexes **1** and **2** are collected in Table 2. Diffraction intensities were collected at room temperature on an Enraf-Nonius CAD4 diffractometer. Due to rapid decay under X-ray exposure, two crystals were used to collect the entire data set for **2** (decay correction range 1.00–2.16 and 1.00–1.26 for the two crystals, respectively). The two data sets were merged and scaled on the basis of the intensities of the 25 reflections used for unit-cell refinement. The unit-cell dimensions were calculated as average values of the two independent determinations. Crystals of **1** were also found unstable, though the rate of decay was not such as to prohibit completion of the data collection (decay correction range 1.00–1.47). Empirical absorption correction was applied for **1** by azimuthal scanning of three reflections with $\chi > 80$ (correction range 1.00–1.23), while the same kind of correction was prevented in **2** by the rapid decay mentioned above. Crystals of **1** and **2** are strictly isomorphous and were it not for a slight, but significant difference in the unit cell volumes [5223 *vs.* 5170 $Å^3$ in **1** and **2**, respectively], and for the spectroscopic evidence described above, data collection for **2** would not have been carried out. Space-group assignment was not unambiguous, several orthorhombic and tetragonal choices

Table 2 Crystal data and details of measurements for complexes **1** and **2**[a]

Complex	**1**	**2**
Formula	$C_{94}H_{60}Au_4O_{20}P_4Rh_{10}\cdot C_5H_9NO$	$C_{92}H_{60}Au_4O_{18}P_4Rh_{10}\cdot C_5H_9NO$
M	3549.45	3493.43
Crystal size/mm	0.10 × 0.12 × 0.15	0.12 × 0.14 × 0.10
a/Å	15.446(3)	15.400(5)[b]
b/Å	15.446(3)	15.400(5)[b]
c/Å	21.894(2)	21.801(5)[b]
U/Å^3	5223	5170
F(000)	3352	3296
D_c/g cm^{-3}	2.17	2.15
μ(Mo-Kα)/cm^{-1}	69.00	69.65
θ range/°	2–20	2.5–25
ω-scan width/°	0.70	1.30
Maximum scan time/s	90	100
Measured reflections	5124	5036
Unique observed [$I_o > 2.5\sigma(I_o)$] reflections (N_o)	2959	2385
Number of refined parameters (N_p)	191	178
R, R',[c] S[d]	0.073, 0.085, 4.37	0.055, 0.063, 1.61
k, g[c]	3.2, 0.0018	1.2, 0.0028

[a] Details in common: tetragonal, space group $P4_2/m$, $Z = 2$, λ(Mo-Kα) = 0.710 69 Å, requested counting $\sigma(I)/I = 0.01$, prescan rate = 8° min^{-1}, prescan acceptance $\sigma(I)/I = 0.5$, octants explored $+h$, $+k$, $+l$. [b] Unit-cell dimensions calculated as average values of two independent determinations (see Experimental section). [c] $R' = \Sigma[w^{\frac{1}{2}}(|F_o| - |F_c|)]/\Sigma w^{\frac{1}{2}}(F_o)$, where $w = k/[\sigma(F) + |g|F^2]$. [d] $S = [\Sigma w(|F_o| - |F_c|)^2/(N_o - N_p)]^{\frac{1}{2}}$.

Table 3 Fractional atomic coordinates for complex **1**

Atom	x	y	z	Atom	x	y	z
Au	0.597 24(6)	0.097 27(6)	0.120 74(4)	O(7)	0.759 5(19)	0.121 0(26)	0.0
Rh(1)	0.561 35(12)	0.061 55(13)	0.0	C(11)	0.854 8(20)	0.199 9(20)	0.217 7(11)
Rh(2)	0.417 11(9)	0.083 11(10)	0.092 61(7)	C(12)	0.944 1(20)	0.189 0(20)	0.211 5(11)
Rh(3)	0.294 82(14)	0.063 43(16)	0.0	C(13)	0.977 0(20)	0.138 8(20)	0.163 9(11)
Rh(4)	0.436 27(16)	0.205 23(14)	0.0	C(14)	0.920 8(20)	0.099 5(20)	0.122 5(11)
P	0.680 7(4)	0.180 6(4)	0.184 4(3)	C(15)	0.831 5(20)	0.110 4(20)	0.128 7(11)
C	0.431 3(18)	0.068 8(16)	0.0	C(10)	0.798 6(20)	0.160 6(20)	0.176 3(11)
C(1)	0.422 7(15)	0.215 5(10)	0.092 5(7)	C(16)	0.630 6(18)	0.080 6(14)	0.286 1(12)
O(1)	0.409 5(13)	0.266 8(11)	0.130 5(7)	C(17)	0.617 6(18)	0.065 4(14)	0.348 2(12)
C(2)	0.285 2(10)	0.080 8(15)	0.092 5(8)	C(18)	0.636 3(18)	0.130 2(14)	0.390 7(12)
O(2)	0.236 8(11)	0.094 3(16)	0.132 8(8)	C(19)	0.667 9(18)	0.210 0(14)	0.371 0(12)
C(3)	0.179 4(11)	0.060 8(33)	0.0	C(20)	0.680 9(18)	0.225 2(14)	0.308 9(12)
O(3)	0.101 4(13)	0.059 7(33)	0.0	C(9)	0.662 3(18)	0.160 5(14)	0.266 4(12)
C(4)	0.432 8(24)	0.084 8(23)	0.137 9(7)	C(21)	0.604 9(18)	0.329 4(17)	0.131 5(13)
O(4)	0.425 7(24)	0.083 5(20)	0.228 8(8)	C(22)	0.591 5(18)	0.418 4(17)	0.126 4(13)
C(5)	0.444 5(34)	0.320 6(12)	0.0	C(23)	0.641 1(18)	0.475 7(17)	0.161 0(13)
O(5)	0.436 3(32)	0.399 2(15)	0.0	C(25)	0.704 1(18)	0.444 0(17)	0.200 8(13)
C(6)	0.567 8(12)	0.194 6(12)	0.0	C(26)	0.717 5(18)	0.354 9(17)	0.205 9(13)
O(6)	0.623 7(23)	0.249 1(20)	0.0	C(8)	0.667 9(18)	0.297 7(17)	0.171 3(13)
C(7)	0.694 0(10)	0.079 0(19)	0.0				

Table 4 Fractional atomic coordinates for complex **2**

Atom	x	y	z	Atom	x	y	z
Au	0.599 76(5)	0.099 82(5)	0.120 35(4)	O(7A)	0.733 9(33)	0.162 1(33)	0.0
Rh(1)	0.560 93(11)	0.060 79(11)	0.0	C(9)	0.853 4(24)	0.179 5(22)	0.224 0(14)
Rh(2)	0.419 18(9)	0.080 83(9)	0.093 18(8)	C(10)	0.942 3(24)	0.163 1(22)	0.219 5(14)
Rh(3)	0.294 85(13)	0.063 46(17)	0.0	C(11)	0.976 2(24)	0.125 6(22)	0.166 4(14)
Rh(4)	0.436 33(16)	0.205 48(13)	0.0	C(12)	0.921 3(24)	0.104 5(22)	0.117 8(14)
P	0.682 7(4)	0.184 2(4)	0.0184 2(3)	C(13)	0.832 4(24)	0.120 9(22)	0.122 3(14)
C	0.431 0(13)	0.068 3(13)	0.0	C(8)	0.798 5(24)	0.158 4(22)	0.175 4(14)
C(1)	0.421 6(14)	0.213 9(17)	0.094 1(12)	C(15)	0.625 2(16)	0.336 6(17)	0.123 0(11)
O(1)	0.410 9(14)	0.267 5(11)	0.131 2(10	C(16)	0.604 9(16)	0.424 4(17)	0.116 7(11)
C(2)	0.281 3(16)	0.759 (14)	0.092 9(12)	C(17)	0.615 8(16)	0.480 7(17)	0.166 2(11)
O(2)	0.229 8(9)	0.087 6(15)	0.131 6(9)	C(18)	0.647 0(16)	0.449 2(17)	0.222 0(11)
C(3)	0.169 7(18)	0.062 1(36)	0.0	C(19)	0.667 2(16)	0.361 4(17)	0.228 3(11)
O(3)	0.099 5(19)	0.057 4(38)	0.0	C(14)	0.656 4(16)	0.305 1(17)	0.178 8(11)
C(4)	0.418 0(17)	0.079 4(18	0.182 3(11)	C(21)	0.480 6(20)	0.128 9(22)	0.281 6(16)
O(4)	0.423 7(19)	0.085 3(17)	0.231 4(10)	C(22)	0.556 7(20)	0.120 0(22)	0.343 1(16)
C(5)	0.442 9(40)	0.328 2(23)	0.0	C(23)	0.613 6(20)	0.146 1(22)	0.389 3(16)
O(5)	0.451 5(38)	0.402 9(23)	0.0	C(24)	0.694 4(20)	0.181 1(22)	0.374 1(16)
C(6A)	0.619 4(47)	0.172 5(47)	0.0	C(25)	0.718 2(20)	0.190 0(22)	0.312 7(16)
O(6A)	0.657 9(29)	0.235 7(30)	0.0	C(20)	0.661 3(20)	0.163 9(22)	0.266 5(16)
C(7A)	0.670 5(33)	0.119 5(33)	0.0				

were found to be compatible with lattice symmetry and extinction conditions. Site symmetries lower than $2/m$ gave ill-defined matrices during refinement. The diffraction pattern was strongly dominated by the highly symmetrical metal-atom frame, the structural model being quite insensitive to the contribution of the light atoms. The final choice fell on the tetragonal space group $P4_2/m$, although some degree of disorder in the phenyl groups orientation (reflected mainly in the large isotropic thermal parameters) could not be avoided. Residual peaks belonging to an independent molecular fragment were found in the Fourier map during the final stages of refinement. They were attributed to the presence of a highly disordered solvent molecule (C_5H_9NO, as shown by elemental analysis, see above). This inference was confirmed by the location of a large cavity (*ca.* 376 Å^3) which might accommodate the solvent molecule. The consistency of the final data sets for **1** and **2**, as well as the solvent-accessible cavity location, was examined with the aid of the computer program PLATON.[11] Since the solvent molecules were highly disordered, it was not possible to add their contribution to the structure model in both **1** and **2**. All atoms except for C(Ph) and H atoms were treated anisotropically in both **1** and **2**. The phenyl rings were refined as rigid groups, with H atoms added in calculated positions (C–H 1.08 Å, C–C–H 120°). The two terminal CO ligands bonded to Rh(1) and Rh(1′) in **2** were found to be disordered over two positions in the equatorial plane. The refinement of an occupancy factor revealed the equivalence of these positions (50% occupancy). For all calculations the computer program SHELX 76[12] was used. Final atomic coordinates are listed in Tables 3 and 4 for **1** and **2**, respectively.

Additional material available from the Cambridge Crystallographic Data Centre comprises H-atom coordinates, thermal parameters and remaining bond lengths and angles.

Acknowledgements

We thank the Ministero dell'Universita' e della Ricerca Scientifica e Tecnologica (MURST) and the Consiglio Nazionale delle Ricerche (CNR) Progetto Finalizzato Chimica Fine II for financial support.

References

1 V. G. Albano, M. Sansoni, P. Chini and S. Martinengo, *J. Chem. Soc., Dalton Trans.*, 1973, 651.
2 A. Fumagalli, S. Martinengo, V. G. Albano and D. Braga, *J. Chem. Soc., Dalton Trans.*, 1988, 1237.
3 V. G. Albano, D. Braga, S. Martinengo, P. Chini, M. Sansoni and D. Strumolo, *J. Chem. Soc., Dalton Trans.*, 1980, 52.
4 B. T. Heaton, L. Strona, S. Martinengo, D. Strumolo, G. Albano and D. Braga, *J. Chem. Soc., Dalton Trans.*, 1983, 2175.
5 V. G. Albano, D. Braga and S. Martinengo, *J. Chem. Soc., Dalton Trans.*, 1981, 717.
6 B. T. Heaton, L. Strona and S. Martinengo, *J. Organomet. Chem.*, 1981, **215**, 415.
7 A. Fumagalli, S. Martinengo, V. G. Albano, D. Braga and F. Grepioni, *J. Chem. Soc., Dalton Trans.*, 1989, 2343.
8 (*a*) V. G. Albano, D. Braga, P. Chini, D. Strumolo and S. Martinengo, *J. Chem. Soc., Dalton Trans.*, 1983, 249; (*b*) D. Strumolo, C. Seregni, S. Martinengo, V. G. Albano and D. Braga, *J. Organomet. Chem.*, 1983, **252**, C93; (*c*) V. G. Albano, D. Braga, D. Strumolo, C. Seregni and S. Martinengo, *J. Chem. Soc., Dalton Trans.*, 1985, 1309.
9 S. Martinengo, D. Strumolo and P. Chini, *Inorg. Synth.*, 1980, **20**, 212.
10 C. Cowala and J. M. Swan, *Aust. J. Chem.*, 1966, **19**, 547.
11 A. L. Spek, PLATON, *Acta Crystallogr., Sect. A*, 1990, **46**, C31.
12 G. M. Sheldrick, SHELX 76, Program for Crystal Structure Determination, University of Cambridge, 1976.

Received 15*th February* 1993; *Paper* 3/00911D